Tellus (2006), 58B, 523–536
Printed in Singapore. All rights reserved

TELLUS

Regional CO_2 fluxes inferred from mixing ratio measurements: estimates from flask air samples in central Kansas, USA

By CHUN-TA LAI[1]*, ANDREW J. SCHAUER[1], CLENTON OWENSBY[2], JAY M. HAM[2], BRENT HELLIKER[3], PIETER P. TANS[4] and JAMES R. EHLERINGER[1], [1]*Department of Biology, University of Utah, 257S 1400E, Salt Lake City, UT 84112-0840, USA;* [2]*Department of Agronomy, Kansas State University, Manhattan, KS 66506, USA;* [3]*Department of Biology, University of Pennsylvania, 415 S University Avenue, Philadelphia, PA 19104, USA;* [4]*National Oceanic and Atmospheric Administration/Climate Monitoring and Diagnostics Laboratory, 325 Broadway, Boulder, CO 80303, USA*

(Manuscript received 20 December 2005; in final form 15 June 2006)

ABSTRACT

We estimated regional fluxes of carbon dioxide (CO_2) using mixing ratios measured in a tallgrass prairie in central Kansas, USA over 3 yr (2002–2004). Glass flasks were used to collect whole air samples in the midafternoon for determining CO_2 mixing ratios and their carbon isotopic composition. Regional CO_2 fluxes were calculated assuming atmospheric boundary layer (ABL) approaches an equilibrium state on a monthly basis. CO_2 mixing ratios derived from the marine boundary layer data were used as a proxy to represent those in the free troposphere, which allowed for determining a boundary layer CO_2 gradient primarily resulting from surface exchange. We estimated temporal changes in the ABL height for this region on a monthly basis (600–1700 m asl for a 5-yr average between 1997 and 2001) from European Center for Medium-Range Weather Forecasts (ECMWF) model data. Accordingly, we estimated the rate of entrainment (flux density) by interpolating NCAR/NCEP reanalysis data to the estimated ABL height. Our study differentiates from previous studies in several aspects: (1) we used flask-based mixing ratio measurements; (2) only discrete midday CO_2 mixing ratio data were used to construct weekly CO_2 gradients between free troposphere and the ABL and (3) we propose a new means for estimating monthly values of vertical transport. Modelled regional CO_2 fluxes were compared to net ecosystem exchange (NEE) of CO_2 fluxes measured by eddy covariance method. Assuming negligible vertical CO_2 gradients between mid-ABL and the surface layer and with no correction applied, calculated NEE showed a general agreement with measured NEE fluxes throughout the growing season. Using CO mixing ratio data, we show that fossil fuel burning contributed negligible CO_2 fluxes in summer but partially explained the discrepancy between modelled regional CO_2 fluxes and measured NEE in winter. This wintertime fossil fuel input was consistent with carbon isotope measurements of CO_2. We demonstrate in this study that CO_2 mixing ratios subsampled at midday in the surface layer can be used to gain insights into regional CO_2 flux exchange in the U.S. Great Plains area.

1. Introduction

The atmosphere integrates surface processes over many temporal and spatial scales and links scalar sources and sinks with concentrations and fluxes via conservation of mass. In a system where momentum fluxes can be described with a closure, atmospheric transport can be treated a priori and the relationship between distribution of sources and sinks, concentrations and fluxes of a scalar can be resolved. In global carbon cycle studies, this mechanism has been inverted to develop inverse models to estimate annual carbon budgets in the terrestrial biosphere at the continental scale (Fan et al., 1998; Rayner et al., 1999; Bousquet et al., 2000; Gurney et al., 2002). Theories of atmospheric transport were also developed to describe scalar transport within plant canopies (Raupach, 1989a,b). One-dimensional biosphere-atmosphere models were subsequently developed to investigate distributions of carbon sources and sinks at the ecosystem scale (Baldocchi, 1992; Baldocchi and Meyers, 1998; Lai et al., 2000a,b; Siqueira et al., 2002).

However, applying the atmospheric model technique to regional spatial scales (roughly defined in the range between 10^4 and 10^6 km^2, see Raupach et al., 1992;Gloor et al., 2001) for

*Corresponding author.
e-mail: lai@biology.utah.edu
DOI: 10.1111/j.1600-0889.2006.00203.x

quantifying annual carbon budgets has been more challenging because at such intermediate scales the atmosphere is often poorly constrained. The atmospheric boundary layer (ABL) has been used as a vehicle to study diurnal carbon dioxide (CO_2) exchange over land (Wofsy et al., 1988; Denmead et al., 1996; Levy et al., 1999; Kuck et al., 2000; Lloyd et al., 2001; Styles et al., 2002). Results from these top-down analyses showed widely variable agreement compared to bottom-up approaches (Fitzjarrald, 2002). The difficulty in applying the ABL budget method on a diurnal timescale resulted from the complex interaction between entrainment, subsidence, cloud effects and horizontal advection.

Reliable methods that are capable of quantifying annual carbon budgets at regional scales are needed in order to understand distributions of carbon sources and sinks on land that were thought to be responsible for the additional atmospheric uptake (Tans et al., 1990; Conway et al., 1994; Ciais et al., 1995; Keeling et al., 1996; Battle et al., 2000). Recently, several studies broke new ground by applying the concept of an equilibrium boundary layer to estimate regional CO_2 fluxes over forest regions (Bakwin et al., 2004; Helliker et al., 2004, 2005). In the context of an equilibrium state, which considers mass and energy exchange in the ABL on timescales longer than a day, subsidence moves airmass downward into the ABL that roughly balances surface fluxes (Betts, 2000; Betts et al., 2004). Synoptic weather events rapidly mix CO_2 in the ABL with the overlying free troposphere (Hurwitz et al., 2004). Focusing on processes that influence the ABL CO_2 budget on monthly timescales, we consider the CO_2 budget equation over monthly means to smooth out large fluctuations resulting from weather disturbance at synoptic timescales. Betts (1992) suggested a simplified ABL CO_2 budget equation, where horizontal advection was assumed negligible compared to vertical transport:

$$\frac{\partial(\rho z C)}{\partial t} = F_c + \rho\left(\frac{\partial z}{\partial t}\right) C_{FT} - \rho W_{FT}(C_{FT} - C), \quad (1)$$

where ρ is the density of air, z is the height of ABL and t is time. F_c is the net surface flux of CO_2, W_{FT} is the mean entrainment rate at the top of ABL (with $\partial z/\partial t = 0$), C represents a well-mixed CO_2 mixing ratio in the ABL and C_{FT} is the CO_2 mixing ratio in the free troposphere. Integrating processes affecting ABL CO_2 mixing ratio on a monthly basis, we applied the concept of an equilibrium boundary layer (i.e. steady-state) and arrived at the following equation (Helliker et al., 2004):

$$\overline{F_c} = \overline{\rho W_{FT}}\,(\overline{C_{FT}} - \overline{C}), \quad (2)$$

where overbar represented time averaging over a month. We noted that the term ρW_{FT} represented a flux density (in units of mol *air* m^{-2} s^{-1}). Flux densities were preferred to the use of a true velocity because flux densities were independent of pressure and temperature and were more readily comparable across sites. If velocity were desired, the vertical variation of air density in the ABL would have to be accounted for (Betts et al., 2004). We will use flux densities to express mean entrainment rates of air into the ABL from the free troposphere throughout this study.

The concept of an equilibrium boundary layer describes the balance between F_c and the CO_2 fluxes across the top of the ABL. This class of ABL approach differs from previous efforts that solved for surface flux of CO_2 through the ABL by increasing the timescale of observation and averaging. Our approach follows the implicit assumption that scalars measured during well-mixed periods in the afternoon capture the mean effect of the diurnal cycle of CO_2 release and uptake. eq. (2) can only be applied, in theory, for processes averaged longer than a day (Betts 2000; Betts et al., 2004; Helliker et al., 2004). This ABL concept has been used to examine regional net CO_2 fluxes in forest regions (Bakwin et al., 2004; Helliker et al., 2004, 2005), but it has not yet been tested in other ecosystem types.

In this study, we adopted eq. (2) to estimate net CO_2 fluxes on a monthly basis in a tallgrass prairie in central Kansas, USA. We performed the ABL budget calculation using mixing ratios subsampled in the midafternoon for 3 yr. Carbon isotope ratios also were determined to discern biological and fossil fuel influences on the surface CO_2 exchange. Calculated net CO_2 fluxes were compared to tower-based eddy flux measurements. The primary objectives of this study were to: (1) evaluate eq. (2) in grassland ecosystems and (2) assess the robustness of subsampling CO_2 mixing ratios in midday for regional estimates of surface fluxes.

Measurements of carbon isotope ratios of atmospheric CO_2 provide additional insights into understanding terrestrial C cycling. Plant organic matter is depleted in the ^{13}C content relative to atmospheric CO_2 because plants discriminate against ^{13}C during photosynthesis (Farquhar et al., 1989). Meanwhile, the atmosphere becomes enriched in ^{13}C contents simply due to mass balance. Much of the ^{13}C-depleted organic products are released back to the atmosphere through ecosystem respiration at night, causing atmospheric ^{13}C contents to decrease. The contrasting effect between photosynthesis and respiration provides isotopic imprints that complement mixing ratio observations for studying biological controls of ecosystem C fluxes. Anthropogenic CO_2 input tends to differentiate from biogenic processes with respect to stable carbon isotope ratios, with the magnitude of discrepancy depends on the type of fuels consumed. Aside from evaluating the ABL approach for regional CO_2 flux estimates, we will also use carbon isotope measurements to address the seasonal influence of biogenic versus fossil fuel derived emissions on CO_2 fluxes in this grassland.

2. Materials and methods

2.1. Study site

Our study site is in the Rannells Flint Hills prairie near Manhattan, Kansas USA (39°12′N, 96°35′W, 324 m asl). The vegetation was dominated by C_4 grass species, primarily *Andropogon gerardii*, *Sorghastrum nutans* and *Andropogon scoparius*. The

C_3 grass and herbaceous species included *Carex* sp., *Vernonia baldwinii, Artemesia ludoviciana, Ambrosia psilostachya and Psoralea tenuiflora* var. *floribunda.* This site was burned annually during the last 10 d of April, and had not been grazed since 1997. The 15-yr average annual precipitation is 878 mm, with 74% occurring between April and September.

An open-path eddy covariance system, consisting of a sonic anemometer (CSAT3, Campbell Scientific Inc., Logan, UT, USA) and a CO_2/H_2O gas analyser (LI-7500, LI-Cor Inc., Lincoln, NE, USA), measured fluxes of momentum, CO_2, sensible and latent heat above the canopy following standard guidelines of the AmeriFlux network (Ham and Heilman, 2003; Lai et al., 2003). Windy conditions generally prevailed at this site, with calm nights representing 0.1% of all the sampling times. Hence, no correction was necessary to account for potential flux loss in low turbulent conditions at night.

2.2. Air sample collection

Lai et al. (2003, 2005) described the protocol of flask air sampling in detail. Briefly, whole air samples have been collected once per week using an automated sampling system (Schauer et al., 2003) with 100 ml flasks (Kontes Glass Co., Vineland, NJ) since March 2002. Two flasks were collected 5 min apart in the midafternoon (halfway between solar noon and sunset; usually between 2:30 and 3:30 p.m. LST) from an intake installed 3 m above ground level (three to six times of canopy height). Sampling at midafternoon takes advantage of strong convective mixing that results in minimum vertical gradients of the ABL CO_2 profile (Bakwin et al., 1998a; Yi et al., 2001). Measurements from this flask pair were averaged to represent midday CO_2 mixing ratio and $\delta^{13}C$ value in the surface layer (Lai et al., 2004, 2005). Flask pairs were evaluated by comparing differences in mixing ratios and isotope composition (details described in Section 2.3). Beginning in March 2003, an extra pair of midafternoon flasks was collected on a separate day every week. Flasks were sealed with vacuum-tight Teflon stopcocks. Air was dried by flowing through a magnesium perchlorate trap before collection. Flasks were collected the day after sampling. All the air samples were then shipped to the Stable Isotope Ratio Facility for Environmental Research at the University of Utah for laboratory analyses.

2.3. Laboratory analyses and data control

CO_2 mixing ratios were measured to a precision of 0.3 ppm using a bellow/IRGA system in 2002 (Bowling et al., 2001; Lai et al., 2003). Carbon isotope ratios of CO_2 were analysed on a continuous-flow isotope ratio mass spectrometer (Finnigan MAT 252, San Jose, CA) with a precision of 0.12‰ for $\delta^{13}C$ (Schauer et al., 2003). Beginning in 2003, an automated GC-IRMS system was deployed to analyse $\delta^{13}C$, $\delta^{18}O$ and mixing ratio of atmospheric CO_2 within each single flask (Schauer et al., 2005). Instrument precision was determined to be 0.48 ppm for CO_2 mixing ratio and 0.06‰ for $\delta^{13}C$ (Schauer et al., 2005). Precision of the automated GC-IRMS system significantly improved isotope ratio analyses (by $\sim$ 0.05‰ for $\delta^{13}C$) but slightly degraded the precision for CO_2 mixing ratio (by $\sim$0.2 ppm). The accuracy of CO_2 mixing ratio measurements, however, was improved due to increased number of standard gas cylinders used for calibration. The automated system used five CO_2 mixing ratio standards (330–550 ppm) that were calibrated against five primary standards (cylinder serial numbers: CC153217, CC153264, CC163396, CC163398 and CC163466) that were measured by WMO Central Calibration Laboratory for CO_2, located at NOAA/CMDL in Boulder, CO, USA. We report carbon isotope ratios relative to the VPDB scale (Coplen, 1996).

Data screening was carefully performed based on both measurements of CO_2 mixing ratio and $\delta^{13}C$. Measurements were excluded from time-series analysis if the standard deviation between the two members of a flask pair exceeds more than five times of instrument precision, which is: (1) the standard deviation in CO_2 mixing ratio between the two members of a flask pair exceeds 2.5 ppm and (2) the standard deviation in $\delta^{13}C$ value between the two members of a flask pair exceeds 0.3‰. 14% of the samples were excluded on this basis.

3. Results

3.1. Time-series of CO_2 mixing ratio and $\delta^{13}C$

A major difference between this study and previous efforts for the quantification of regional net CO_2 fluxes is the sampling method of acquiring mixing ratio data. Helliker et al. (2004) and Bakwin et al. (2004) both used IRGA-based CO_2 mixing ratio data to infer regional net CO_2 fluxes. Their mixing ratio data are continuous and more frequent (half-hourly averages) compared to flask-based measurements. Measurements with air samples in flasks, despite having the advantage of providing additional information regarding the associated isotopic composition of the same airmass that was analysed to determine its mixing ratios, are discrete in time. In our case, time-series of CO_2 mixing ratios and $\delta^{13}C$ values in the surface layer were constructed from 16 to 20 measured values every month. These measurements, although consistently sampled at midafternoon throughout a year when convective mixing was the strongest, presented a legitimate concern as to whether we adequately captured important mass exchange events that most likely to impact the seasonal pattern of surface photosynthesis and respiration.

Figure 1 shows the seasonal pattern of observed CO_2 mixing ratios and $\delta^{13}C$ values from analyses of midafternoon air samples collected in the Rannells prairie. The distinct seasonal characteristics resulting from the contrasting forcing of photosynthesis and respiration by surface vegetation was clearly detectable. The seasonal pattern in CO_2 mixing ratio and $\delta^{13}C$ mirrored each other, reflecting the influence of surface biological activities. The

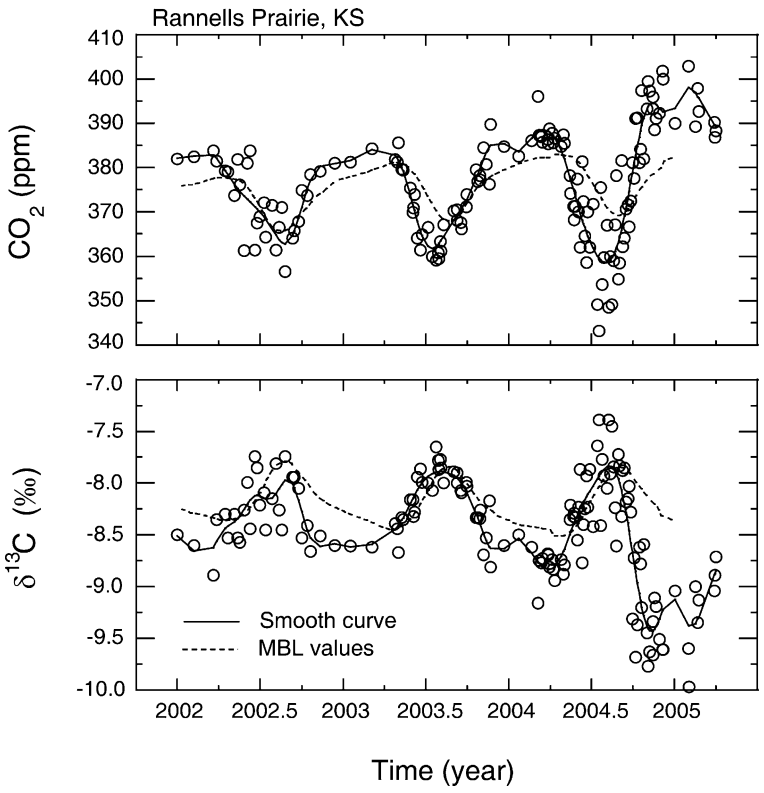

Fig. 1. Mixing ratios and $\delta^{13}C$ of CO_2 in the surface layer measured in the midafternoon. Open circles represent samples collected 3 m above ground fitted with a smooth curve (solid line). Also shown are values in the free troposphere (dash-line), represented here by MBL reference matrices derived from measurements within NOAA/CMDL network.

seasonal swing ranged between 20 and 35 ppm for CO_2 mixing ratio and 1–1.5‰ for $\delta^{13}C$ between years, with larger intraannual fluctuation in 2004.

Superimposed on the measurements were smooth curve fittings and free tropospheric values represented by data derived from marine boundary layer (MBL) measurements (Masarie and Tans, 1995). MBL data (in the case of CO_2 matrix, see Globalview-CO_2, 2003) were extracted to represent free tropospheric values for the same latitude as our study site. For the rest of the paper, we assumed that MBL data are reasonable proxies to represent free troposphere in the study area. Analyses that incorporate experimental data have contributed to the justification of adopting this assumption. Yi et al. (2004) used measurements from a tall tower in Wisconsin, USA to demonstrate that differences in CO_2 mixing ratios between convective boundary layer and MBL are much larger than those measured between the MBL and the free troposphere. Their observations reassure the use of the MBL reference for terrestrial CO_2 flux studies. Bakwin et al. (2004) used both MBL proxies and aircraft measurements to represent the free troposphere in their calculation of regional CO_2 fluxes. They showed a general agreement between the two estimates at three out of the four study sites. In the absence of continuous measurements from the free troposphere, we also used MBL reference in the current study. Examples that used MBL data as proxies also include analyses that calculated regional CO_2 fluxes (Helliker et al., 2004) and canopy-scale photosynthetic discrimination against ^{13}C (Lai et al. 2004, 2005).

We used the method described by Thoning et al. (1989) for smooth curve fitting. The curve fit function consists of a second-order polynomial and two annual harmonics. Relative to the free troposphere, measurements in the surface layer exhibited greater seasonal fluctuations. The difference between tower observations and the free troposphere reflected the combined influence of surface vegetation and atmospheric transport.

When the CO_2 difference (surface layer minus free troposphere) was averaged on a monthly basis (Fig. 2), seasonal CO_2 evolution was remarkably different among the 3 yr. Lai et al. (2006) showed that the productivity and the carbon and oxygen isotope ratios of respiration differed substantially in this tallgrass prairie because of contrasting water availability among the 3 yr. Total precipitation between April and September was 494, 653 and 746 mm in 2002, 2003 and 2004, respectively. Compared to the 15-yr average of 649 mm, the 3 yr represent a drought, an average and a wet year, respectively. A record low precipitation input (∼10 mm) was received in June of 2002 (Lai et al., 2003). This was only 8% of the total rainfall received for the same month averaged over 15 yr. By contrast, twice the average rainfall was received in June of 2004. Spring precipitation has the largest impact on productivity because the primary growth period for tallgrass prairie is during the first half of the season. Reduced (enhanced) gross CO_2 uptake by surface vegetation resulted in the contrasting seasonal pattern of CO_2 mixing ratio in the surface layer relative to the free troposphere (Fig. 2).

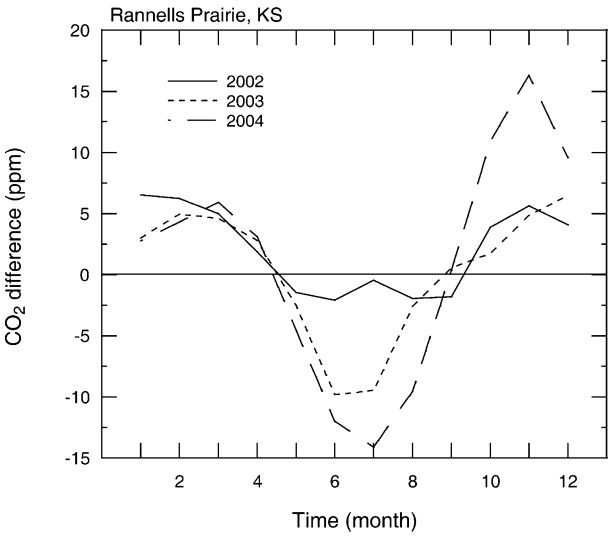

Fig. 2. Monthly averages of CO_2 difference (surface layer minus free troposphere). The 3 yr represent a dry, an average and a wet year with respect to growing season water conditions in 2002, 2003 and 2004, respectively.

Our midafternoon samples provide no information regarding diurnal cycles of CO_2 exchange between land surface and the overlying atmosphere. Our interest is to depict an ensemble, longer than diurnal averaging of CO_2 mixing ratios and fluxes in the context of an equilibrium boundary layer. By subsampling midafternoon air, we were able to describe a great deal of seasonal characteristics of atmospheric CO_2 and $\delta^{13}C$ in the surface layer and that of ABL. The seasonal pattern shown in Fig. 2 was very similar to those shown by IRGA-based measurements in forest regions (Bakwin et al., 1998a, 2004; Helliker et al., 2004, 2005; Hurwitz et al., 2004; Davis, 2005). This similarity implies the eminent role of large-scale atmospheric transport in the ABL CO_2 budget and the feasibility of adopting a subsampling scheme that measures CO_2 mixing ratios consistently from midafternoon air samples. However, a small vertical gradient (1–2 ppm) exists between CO_2 measurements taken in tall towers and flux towers (Bakwin et al., 1998a; Yi et al., 2001). Empirical corrections for this vertical gradient have been proposed (Davis et al., 2000; Davis, 2005). We do not explicitly account for the CO_2 gradient in the calculation of regional fluxes, but we will examine the impact of this gradient on the estimate of regional fluxes with a sensitivity analysis.

3.2. Boundary layer height

The height of the ABL has a strong diurnal evolution. After sunrise, surface heating from solar radiation results in convective mixing that entrains air from the residual boundary layer into a mixed layer. The mixed layer feeds off the entrainment from overlying air and continues to grow until it reaches a maximum height in the afternoon. This capping of the air column, resulting from the inversion of potential temperature and specific humidity, defines the height of ABL, which is relatively easily identifiable when a high-pressure system persists with large-scale subsidence. After sunset, the ABL quickly collapses in the absence of convective turbulence and a stable boundary layer forms during the night (Stull, 1988).

The height of the ABL top is needed to determine the vertical transport where free tropospheric air is entrained into the ABL during convective mixing. For the current study, we do not have direct measurements of the ABL height. We rely on information from the European Center for Medium-Range Weather Forecasts (ECMWF) reanalysis model data (ECMWF ERA-40, http://www.ecmwf.int/) to estimate temporal changes in the ABL height for the study area. At the time of this analysis, the ECMWF ERA-40 data have been released to the public for periods prior to August 2002, but data for the majority of our study period were not yet available. To gain some understanding of how ABL height varies seasonally, we used ECMWF ERA-40 data between 1997 and 2001. We extracted modelled values from daily fields in the ECMWF ERA-40 data to estimate the maximum height of a diurnal ABL (at 12:00 p.m. local time). On this basis, we calculated monthly averages of maximum ABL height for a grid (40°N and 97.5°W) that is closest to our study site using data from the previous 5 yr (1997–2001) of the study period (Fig. 3). The modelled ABL heights revealed a large seasonal difference. The maximum ABL height ranges between 600 m in January and 1800 m in May. Each of the 5 yr showed a similar seasonal pattern. Hence, we calculated a composite estimate of the ABL height over a year (the thick line in Fig. 3), and used this long-term average to derive flux densities in the calculation of regional CO_2 fluxes.

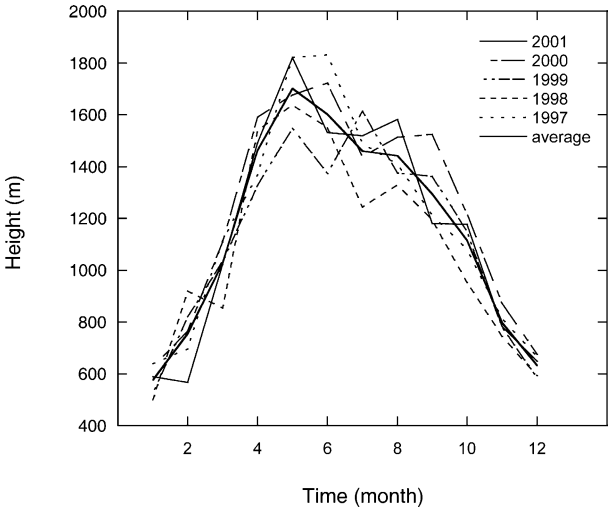

Fig. 3. Modelled maximum ABL height (metres, asl) for the study area in the ECMWF ERA-40 data product. The thick line represents a composite estimate of the ABL height averaged over 5 yr.

3.3. Flux density

The rate of exchange between the free troposphere and the ABL (expressed as flux density, ρW_{FT}) is critical to the calculation of regional CO_2 fluxes. Different methods have been proposed to estimate ρW_{FT}; Helliker et al. (2004, 2005) used water vapour flux and mixing ratio measurements to estimate ρW_{FT}; they then applied ρW_{FT} to CO_2 exchange by assuming a similarity between CO_2 and water vapour transfer. Bakwin et al. (2004) used NCAR/NCEP reanalysis model data (Kalnay et al., 1996; http://www.cdc.noaa.gov/cdc/reanalysis/) to estimate W_{FT}, for which they derived regional CO_2 fluxes and compared to tower-based eddy covariance fluxes.

The method used by Helliker et al. (2004, 2005) requires information about water vapour mixing ratios in the free troposphere, which we do not have. ECMWF modelled ρW_{FT} estimates are not yet available for our study period. We assume NCEP reanalysis reasonably resolves vertical transfer for the region. To investigate how trustworthy this assumption was, we compared monthly means of daily ρW_{FT} values at two heights from the grid at 40°N, 95°W over 2 yr (2000 and 2001) between ECMWF and NCEP reanalysis data (Fig. 4). Both modelled ρW_{FT} values show very similar seasonal patterns and generally agree within less than 0.1 mol m^{-2} s^{-1} on monthly means. This agreement between two independent ρW_{FT} estimates provides supports of using NCEP reanalysis ρW_{FT} in this region, where surface geometry is relatively flat and ideal for simulating atmospheric transport (see the First ISLSCP Field Experiment, FIFE project description via: http://www.esm.versar.com/fife/fifehome.htm).

Flux densities in large-scale models are forced by horizontal convergence. When ρW_{FT} values are averaged over a long period (e.g. a month), the mean state should become close to zero since otherwise a net divergence or convergence will result. As shown in Fig. 4, monthly means of daily ρW_{FT} values fluctuate around zero. Bakwin et al. (2004) estimated W_{FT} as monthly means of the *absolute* value of daily vertical velocity. Their approach increased the magnitude of monthly averaged W_{FT} values, but no physical interpretation was given as to why absolute values of daily W_{FT} were used.

We computed monthly averages of ρW_{FT} by a new approach. We calculated ρW_{FT} by including only *negative* daily ρW_{FT} values. Our rationale for including only negative (subsidence) daily ρW_{FT} values is in accordance with the equilibrium boundary layer concept, which assumes that the ABL reached a steady-state between surface fluxes, cloud effects on radiation and subsidence of the overlying free troposphere when averaged over timescales longer than a day (Betts and Ridgeway, 1989; Betts, 2000). This assumption is more likely to be valid when high-pressure system prevails, in which case entrained air (negative vertical transport) allows the ABL to grow. Helliker et al. (2004, 2005) showed that by including only values in fair-weather conditions (when subsidence dominates), the magnitude of ρW_{FT} increased and estimates of regional CO_2 fluxes in general had a better agreement with tower flux measurements. The inclusion of only negative ρW_{FT} is analogous to the argument of constraining the analysis to fair-weather conditions.

On this basis, we first extracted ρW_{FT} values from the NCEP reanalysis data. We then interpolated NCEP reanalysis ρW_{FT} values to the top of the ABL height, using the composite curve (thick line) shown in Fig. 3. Consequently, the seasonal variability of the ABL height was accounted for in our monthly estimates of ρW_{FT} (Fig. 5). This is a new aspect that differs from previous studies in which the seasonality in the boundary layer height has not been accounted for. A maximum downward flux density

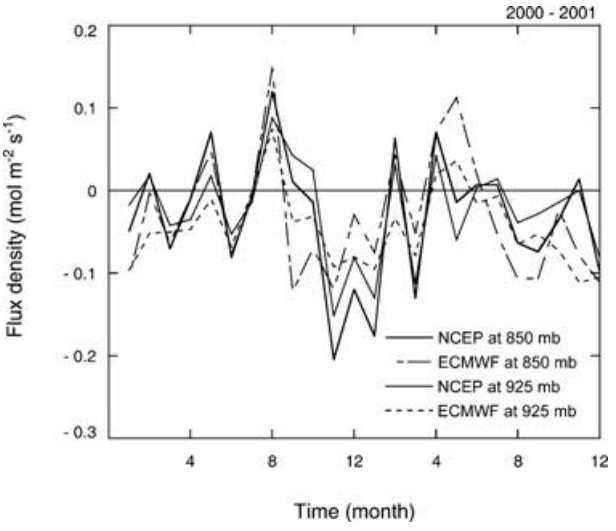

Fig. 4. Comparison of the flux density (ρW_{FT}) at two different heights extracted from NCAR/NCEP reanalysis and ECMWF ERA-40 database.

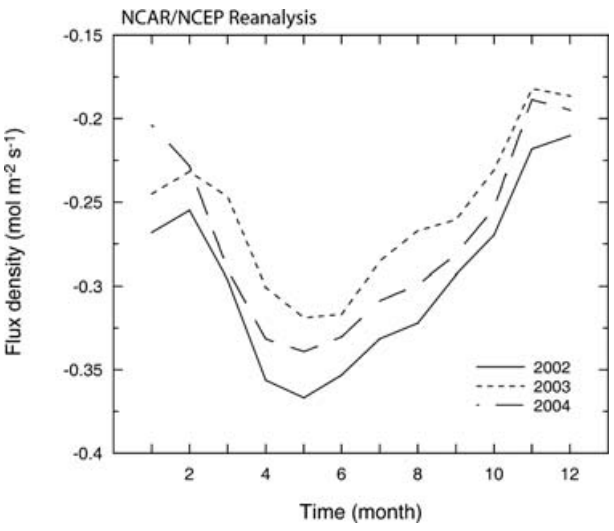

Fig. 5. Monthly averages of the flux density extracted from the NCAR/NCEP reanalysis data used in the calculation of regional CO_2 fluxes.

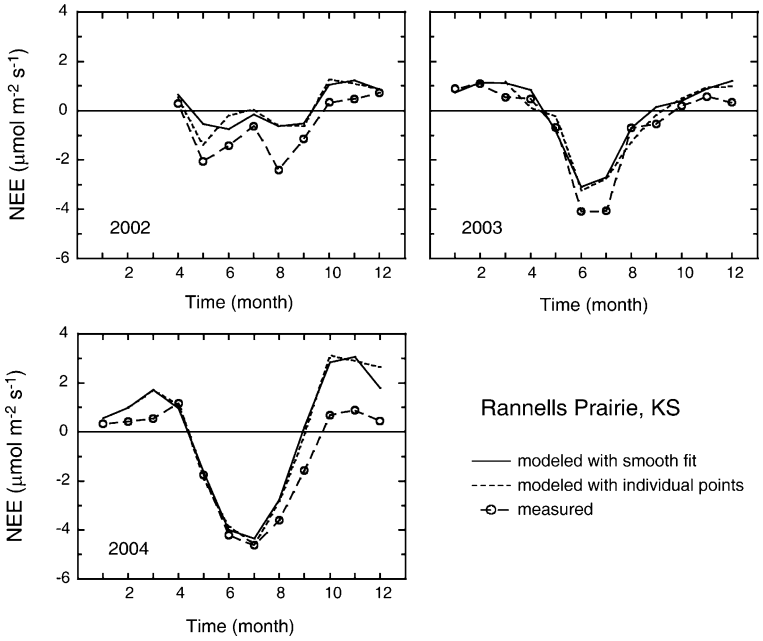

Fig. 6. Comparison between modelled regional CO_2 fluxes and local flux measurements by eddy covariance method. Both modelled and measured CO_2 fluxes were presented as monthly averages. Modelled CO_2 flux estimates were calculated using CO_2 differences between free troposphere and (1) smooth curves (solid line) and (2) individual air samples (dash-line).

appears in May on annual timescales, which is consistent with the timing of the peak in the modelled ABL height from the ECMWF data.

3.4. Comparison of net CO_2 fluxes

Differences in CO_2 mixing ratios between the surface layer and the free troposphere (Fig. 2) and ρW_{FT} estimates (Fig.5) allow for computing net ecosystem exchange (NEE) of CO_2 fluxes on a monthly basis. Due to the large surface area ($\sim 10^6$ km^2) that contributes to variations in mixing ratio measurements (Gloor et al., 2001), calculated NEE likely represent CO_2 exchange on a regional spatial scale. On the other hand, tower-based flux measurements usually cover a source area (much) less than a few kilometres. Hence, one should not expect agreements when comparing calculated NEE with eddy covariance measurements.

Figure 6 shows the comparison between modelled and measured NEE averaged over monthly timescales for the 3 yr. Here negative fluxes represent carbon uptake by the prairie. There were substantial differences in measured NEE fluxes between years, mainly reflecting the effect of soil water availability on the carbon transfer in this grassland (Lai et al., 2006). The net carbon uptake was the lowest in the summer of 2002, with a significant midsummer reduction due to drought. The drought caused daily sums of NEE flux to be nearly neutral during this period (Fig.6; also see Lai et al., 2003). By contrast, net uptake of atmospheric CO_2 was the greatest in the 2004 growing season, a wet year with little water limitation.

For all 3 yr, calculated NEE showed a generally satisfactory agreement describing the rate of CO_2 change with respect to measured NEE fluxes during the growing season. To test the effect of smooth curve fitting, NEE fluxes were calculated using CO_2 differences between the free troposphere and (1) smooth curves (solid lines) and (2) individual air samples (dash-lines). Figure 6 shows that the effect of smooth curve fitting is small. When comparing calculated and measured NEE fluxes, there were obvious discrepancies about 1–2 μmol m^{-2} s^{-1} regarding peak rates of net uptake in 2002 and 2003. Calculated NEE was also lower than tower measurements in the second half of 2004. Nevertheless, calculated NEE appeared to successfully capture seasonal fluctuations of measured NEE fluxes during each of the 3 yr. In particular, derived regional NEE fluxes resemble the depression of midsummer NEE in 2002, when a severe drought occurred and substantially reduced photosynthetic uptake in grassland in central Great Plains. This drought response was observed by tower NEE measurements (Lai et al., 2003), which represented a relatively small area. One could not draw conclusions as to whether such a response applied to a larger spatial region solely based on tower data. Figure 6 provides evidence that the tower NEE measurements in Rannells prairie are representative of general flux patterns that occur at the regional scale. This is quite remarkable given that similar agreements exist between measured and derived NEE for all 3 yr that represent very different growing conditions with contrasting soil moisture contents. The importance of these results and their implication to regional carbon studies will be further discussed later.

3.5. Effects of fossil fuel emission

Calculated NEE fluxes from mixing ratio data represent a much greater spatial area, likely including contributions of both biogenic and anthropogenic components from a regional spatial

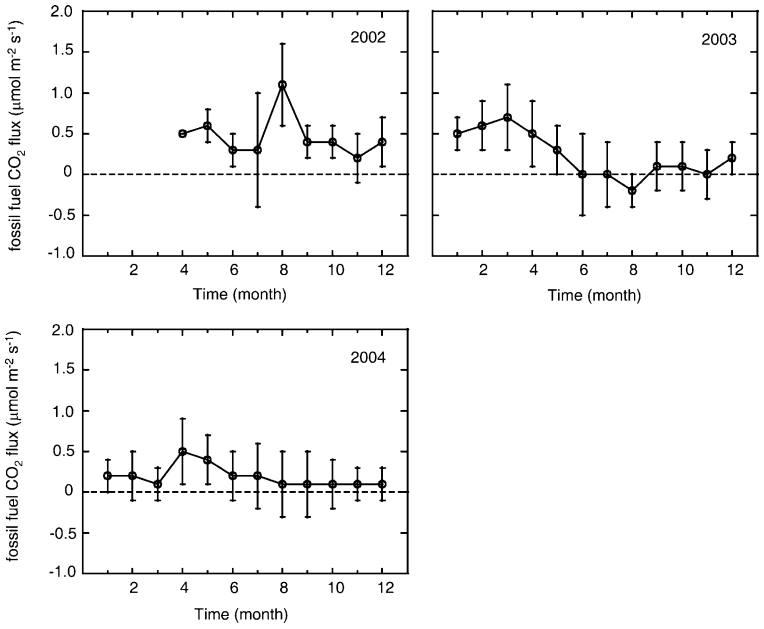

Fig. 7. Regional fossil fuel fluxes of CO_2 estimated from CO data measured at the Southern Great Plains Station, Oklahoma, USA (36.8°N, 97.5°W) within the NOAA/CMDL network. Error bars indicate one standard deviation, propagated through errors in the monthly means of the CO measurements.

scale. Tower measurements represent relatively local CO_2 exchange in a managed, ungrazed grassland. The calculated NEE fluxes were consistently greater in winter. This discrepancy can be partially explained by the fossil fuel emission in the region that contributes to the mixing ratio data, which consequently increases calculated NEE fluxes in winter. Although fossil fuel emission also affects summertime CO_2 fluxes, its effects are usually much smaller and negligible (Bakwin et al., 2004).

Because mixing ratios of carbon monoxide (CO) were not measured at our flux tower, we used CO mixing ratios measured at the Southern Great Plains (SGP) Station, Oklahoma, USA (36.8°N, 97.5°W) within the NOAA/CMDL network to obtain a sense of the magnitude of fossil fuel CO_2 fluxes for the region. We used an emission ratio of 20 (CO ppb/CO_2 ppm) to estimate fossil fuel-derived CO_2 from CO measurements (Bakwin et al., 1998b). Regional estimates of anthropogenic CO_2 fluxes were calculated with CO data from the SGP station, by using eq. (2) and MBL CO values from the NOAA/CMDL network. Results were shown in Fig. 7. Figure 7 suggests that fossil fuel CO_2 emission was generally greater in winter, and perhaps was negligible in summer as indicated in 2003 and 2004. Taking into account the fossil fuel CO_2 fluxes, however, only partially explains the discrepancy between calculated and measured NEE fluxes. For example, the large discrepancy ($\sim$2 μmol m^{-2} s^{-1}) occurred in October and November of 2004 cannot be solely explained by fossil fuel CO_2 fluxes.

Measurements of carbon isotope ratios from whole air samples can be used to examine the relative importance of the role of biogenic exchange and anthropogenic emission in regional CO_2 fluxes. Considering canopy-atmosphere CO_2 exchange under daytime conditions, δ^{13}C values associated with net CO_2 fluxes ($\delta^{13}C_{net}$) can be calculated from the mass balance equations for total CO_2 and $^{13}CO_2$, given by:

$$C_m = C_t + C_s \qquad \delta^{13}C_m C_m = \delta^{13}C_t C_t + \delta^{13}C_{net} C_s \qquad (3)$$

where C represents CO_2 mixing ratios and subscripts m, t and s represent measurements within the mixed layer (generally speaking but usually within canopies or a few meters above canopies), the troposphere and CO_2 production (consumption) from local sources, respectively. Note that both biogenic and fossil fuel sources can affect CO_2 mixing ratios observed in terrestrial stations (Bakwin et al., 1998b; Potosnak et al., 1999). Bakwin et al. (1998b) separately determined the δ^{13}C value of biological and fossil fuel fluxes by considering the influence of both components using a two-parameter fit model. Here, we calculated $\delta^{13}C_{net}$ values assuming only one process dominates the source term at a time, i.e. biological processes dominate the rate of CO_2 change in summer and fossil fuel emission dominates the rate of CO_2 change in winter. This assumption allows for calculating $\delta^{13}C_{net}$ with a one-parameter fit model, i.e. δ^{13} C $_{net} = (\delta_m C_m - \delta_t C_t)/(C_m - C_t)$. We emphasize that such assumption does not determine $\delta^{13}C_{net}$ values a priori.

Another thing to consider is the atmospheric ^{13}C disequilibrium effect resulting from the δ^{13}C difference between contemporary atmosphere and a past atmosphere under which a fraction of respired carbon was photosynthetically fixed (Fung et al., 1997). The atmospheric δ^{13}C value has been decreasing at a rate of $\sim 0.02‰$ yr^{-1} as a result of the addition of fossil carbon that contains low ^{13}C contents (Trolier et al., 1996). As a result, δ^{13}C values in organic carbon fixed through photosynthesis also are expected to decrease over time. Photosynthates with varying

$\delta^{13}C$ values are transported and stored into different terrestrial carbon pools for various time durations before returning to the atmosphere. Hence, respired CO_2 consists of carbon of different ages (Schimel et al., 1994). The age distribution of carbon during respiration varies with time (days to decades). In grassland ecosystems where patterns of carbon transfer are highly seasonal (Suyker and Verma, 2001), this age difference is likely enhanced between carbon respired in summer and winter.

We have neglected the influence of atmospheric ^{13}C disequilibrium on the seasonal $\delta^{13}C_{net}$ variation in the derivation of eq. (3). What is the seasonal impact on our $\delta^{13}C_{net}$ estimates if we were to consider the disequilibrium effect, given that different ages of carbon contribute disproportionately in summer and winter? Lets consider a simple example to demonstrate this impact. In summer, assuming 80% of respired CO_2 consisting of carbon with an age of less than 2 weeks (0.04 yr). Such fast turnover rates of recently fixed photosynthates have been suggested for grassland ecosystems (Bremer et al. 1998; Craine et al., 1999). We also assume a combined old carbon pool contributes to the other 20 % with an average age of 10 yr (Fung et al., 1997). This gives respired CO_2 fluxes with a weighted age of $0.04 \times 0.8 + 10 \times 0.2 = 2$ yr. In winter, lets assume 50% of respired CO_2 consisting of carbon with an age of 1 yr (e.g. litter decomposition) and 50% of combined old carbon pools (10 yr). The weighted age for respired CO_2 in winter would be $1 \times 0.5 + 10 \times 0.5 = 5.5$ yr.

The seasonal age difference associated with the disequilibrium effect is $(5.5 - 2) \times 0.02‰\,yr^{-1} = 0.07‰$. Therefore, neglecting disequilibrium effect has little influence on the seasonal $\delta^{13}C_{net}$ variation. We can exclude the possibility that atmospheric ^{13}C disequilibrium contribute significantly to the difference in the 'apparent' $\delta^{13}C_{net}$ values between summer and winter.

The CO_2 difference between the free troposphere and the surface layer, $(C_m - C_t)$, which resides in the denominator of the formula that calculates $\delta^{13}C_{net}$ results in a numerical instability whenever this term approaches zero. On an annual basis, this tends to occur in the spring (April) and fall (September) as shown in Fig. 2. For this reason, values of $\delta^{13}C_{net}$ were not shown for the entire 2002 and in April and September when small CO_2 difference exists.

Figure 8 shows that $\delta^{13}C_{net}$ values differed substantially between growing and non-growing seasons. During the growing season, $\delta^{13}C_{net}$ values appeared to reflect the strong biotic exchange between the atmosphere and the surface vegetation in the region, which is dominated by C_4 photosynthesis. As vegetation became less active, $\delta^{13}C_{net}$ values became more negative, suggesting a change in CO_2 sources that dominate the region. The wintertime $\delta^{13}C_{net}$ values were overly negative compared to values derived from biogenic carbon substrates. It is likely that a greater contribution from fossil fuel emission (e.g. methane-originated fuels for heating) (and perhaps the reduced vertical exchange of air in winter-rectifier effect) results in very negative $\delta^{13}C_{net}$ values for the region.

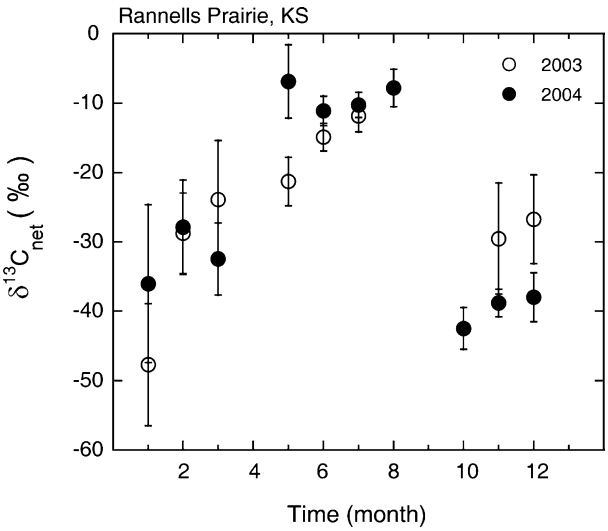

Fig. 8. Monthly estimates of carbon isotope ratios associated with net CO_2 fluxes for 2003 and 2004. Values of $\delta^{13}C_{net}$ were not calculated for 2002 because of the relatively greater uncertainty in CO_2 mixing ratio data (see text).

4. Discussion

In this study, we used CO_2 mixing ratios measured in the surface layer above a grassland to estimate net CO_2 fluxes on a monthly basis. Estimates of the net CO_2 flux were likely representative of a regional spatial scale owing to the large source area that affects mixing ratio data (Gloor et al., 2001). The boundary layer budget approach was rigorously tested using measurements in a grassland over 3 yr of contrasting water conditions, and we found remarkable agreements between modelled and measured NEE fluxes. Despite of many simplifications and assumptions, such as neglecting the vertical CO_2 gradient within the mixed layer, we found the equilibrium ABL method quite successful. These results should provide a basis for refinement in future work in this field. Other studies also showed that mixing ratios in the ABL are correlated with synoptic passages so that one can infer surface fluxes with a relatively simple calculation from mixing ratio measurements (Bakwin et al., 2004; Betts et al., 2004; Helliker et al., 2004; Hurwitz et al., 2004; Yi et al., 2004).

The ABL budget approach defines CO_2 gradients between mixing ratios in the free troposphere and those from a well-mixed boundary layer, which is usually achieved when strong convective mixing presents. CO_2 mixing ratios, when evaluated at midday over land, are fairly constant over the entire air column in the ABL (Yi et al., 2001). The vertical mixing ratio gradients within the continental ABL are quite small (Stull, 1988; Moeng and Wyngaard, 1989), which has been verified by tall tower measurements (Bakwin et al., 1998a; Yi et al., 2001). However, a small vertical gradient of CO_2 mixing ratio may still exist between mid-ABL and the surface layer. Davis (2005) showed that CO_2 mixing ratios measured at 396 m and 30 m differed by

Table 1. Monthly values of modelled net CO_2 fluxes (F_c), measured NEE fluxes, and corrected net CO_2 fluxes by adjusting CO_2 mixing ratio differences between the surface layer and mid-ABL (see text) for the 3 yr. All terms are in units of μmol m^{-2} s^{-1}

Month	2002			2003			2004		
	F_c	Measured	Corrected	F_c	Measured	Corrected	F_c	Measured	Corrected
1				0.7	0.9		0.6	0.3	
2				1.1	1.1		1.0	0.4	
3				1.1	0.5		1.7	0.5	
4	0.7	0.3		0.8	0.5		1.0	1.2	
5	−0.5	−2.1		−0.8	−0.7		−1.6	−1.8	
6	−0.7	−1.4	0.7	−3.1	−4.1	0.6	−4.0	−4.2	0.7
7	−0.2	−0.6	0.7	−2.7	−4.1	0.6	−4.3	−4.6	0.6
8	−0.6	−2.4	0.6	−0.7	−0.7	0.5	−2.8	−3.6	0.6
9	−0.5	−1.1	0.6	0.1	−0.5	0.5	0.2	−1.6	0.6
10	1.0	0.3		0.4	0.2		2.8	0.7	
11	1.2	0.5		0.9	0.6		3.1	0.9	
12	0.9	0.7		1.2	0.3		1.8	0.5	

0–2.2 ppm (with larger difference occurring between June and August) on a monthly basis for measurements at the WLEF tall tower in Wisconsin in 1997. Such CO_2 mixing ratio difference between the surface layer and mid-ABL, when compared to the seasonal amplitude of continental ABL and the difference between marine and continental boundary layers, is much smaller. As a result, subsampling CO_2 mixing ratios and fluxes in mid-day convective conditions in the surface layer provide useful information for studying terrestrial carbon cycles (Davis et al., 2005).

Davis (2005) described a flux-gradient method to correct for the small CO_2 vertical gradient between the surface layer and mid-ABL. According to Davis (2005), the correction varies linearly with the magnitude of the surface flux; hence, no correction is required when fluxes are small (i.e. winter). Because the flux-gradient method has only been tested against measurements at the WLEF tower, and uncertainties with the method have been documented (Davis et al., 2005), we did not include this small correction in our regional estimates of net CO_2 fluxes. This bias is mostly likely to influence calculations for the summer months. We performed a sensitivity analysis to simulate a correction of 2 ppm (mid-ABL minus surface layer), and re-calculated the net CO_2 fluxes for months between June and September. The results were summarized in Table 1.

We remain cautious when interpreting results from the sensitivity simulation. We emphasize that no actual measurements are available to suggest a 2-ppm difference between mid-ABL and the surface layer for the study region. Based on WLEF tower studies (Davis, 2005), this magnitude represents the greatest difference that occurs in summer. To simulate a maximum impact that servers as an upper bound of ignoring a potential CO_2 vertical gradient on the net CO_2 estimate, we chose the same 2 ppm difference as that reported for a forested area. We also simplify the calculation by assigning a constant CO_2 difference, as opposed to scaling the difference with surface fluxes (Davis, 2005). The sensitivity test performed here should not strictly be regarded as a true correction, but it should at least provide a qualitative assessment.

When CO_2 mixing ratio gradient was considered, net uptake of CO_2 fluxes based on the ABL approach generally decreased by 0.5–0.7 μmol m^{-2} s^{-1} in summer, when the correction is most likely to be important. The impact of this correction should be viewed approaching an upper bound based on studies from WLEF tower. Our simple calculation also suggests that the correction does not substantially affect model's ability to depict the rate of change in measured NEE fluxes.

Complete agreement between measured NEE and calculated net CO_2 fluxes was not expected because of the difference in spatial scales the two quantities represent. Given the heterogeneity of land uses in the area (mixtures of natural tallgrass prairie with agricultural crop fields), it is not too surprising that regional and local estimates of NEE fluxes do not fully agree in magnitude. It is interesting to point out that calculated net CO_2 fluxes achieved better agreements with measured NEE when we considered mixing ratios in the surface layer. Without knowing the actual CO_2 gradients in the mixed layer for the region, we do not know whether this agreement is only a coincidence. This is an issue that needs to be addressed in future studies. What is more important, perhaps, is the rate of change in NEE fluxes, which is relatively well described by the ABL method. The timing of the transition from a positive rate of change to a negative rate of change and vice versa is determined primarily by biotic factors (e.g. bud break and senescence), as well as anomaly in weather patterns. It is important to identify whether such biotic controls occur at a large spatial scale. For example, regional estimates of NEE showed a reduced net uptake during the drought event

in July 2002, consistent with tower flux measurements. This regional phenomenon has important ecological and agricultural implications.

Because subsiding circulation dominates in fair weather conditions, derived CO_2 fluxes should be strictly compared to the NEE measured in the same condition. In this study, we did not exclusively separate flux data from rainy days because we have filled missing data from wet periods with using a diurnal mean cycle gap-filling approach (Falge et al., 2001). This gap-filled strategy replaces a missing datapoint from a specific time of day with the diurnal mean for the same time computed using a 7–14-d moving window that is time-centred around the missing point. Thus, periods of inclement weather are replaced with the mean from periods having more favourable conditions. This gap-filling strategy has a minor effect on the calculated annual carbon fluxes in this plains ecosystem because precipitation is infrequent and tends to occur in a few discrete events.

The selection of ρW_{FT} is critical to the calculation of regional CO_2 fluxes. In the context of an equilibrium boundary layer, when averaged over periods longer than the diurnal cycle, surface fluxes are nearly in balance with large-scale subsidence when the cloud effects on radiation are negligible (Betts and Ridgeway, 1989; Betts, 2000). In the current study, we selected only negative daily ρW_{FT} values when subsidence dominates. This choice can be viewed analogous to the argument by including only fair-weather conditions, but is stricter than using precipitation as the dependent variable. For example, further screening ρW_{FT} values by excluding rainy days results in exactly the same monthly ρW_{FT} averages.

Bakwin et al. (2004) estimated W_{FT} as monthly means of the *absolute* value of daily vertical velocity from the NCEP reanalysis data. Without taking absolute values, monthly averages of daily ρW_{FT}would have been very close to zero, resulting in very small net CO_2 fluxes. When comparing the approach of Bakwin et al. (2004) with the current study, our proposed method results in only slightly smaller (more negative) ρW_{FT} values. This difference, much smaller than vertical gradients between, for example, ρW_{FT} values at 700 and 850 mb levels, results from the fact that monthly averages of daily ρW_{FT} value approach zero. Hence, positive and negative ρW_{FT} values roughly equal to each other, resulting in little net effect from taking absolute values.

It is possible that we have underestimated actual ρW_{FT} by relying on large-scale atmospheric model predictions (e.g. NCEP reanalysis or ECMWF ERA-40 data) to estimate vertical transport because subgrid processes were not considered. Cotton et al. (1995) estimated turnover time of the ABL air about 4 d on a global average. Continuous measurements of the boundary layer height or of residence time of air in the ABL between synoptic events, critical to understand subgrid processes, are rare. We are not aware of this type of field measurements suitable for the current purpose, which is to examine regional CO_2 exchange at monthly timescales for 3 yr. Alternatively, the approach by Helliker et al. (2004, 2005) can be employed to verify ρW_{FT}, which needs to be more carefully addressed in future work.

CO measurements became available after April 2002 at the SGP station, and those measurements indicated an unusually high CO content in the atmosphere during the 2002 growing season, resulting in relatively high fossil fuel CO_2 fluxes throughout the year. Accounting for this additional CO_2 source partially explains the discrepancy between modelled regional CO_2 fluxes and measured NEE. By contrast, CO measurements in 2003 and 2004 indicate negligible contributions to regional CO_2 fluxes in summer. The spatial distribution of crop fields, presumably supplied with irrigation and therefore with higher productivity, may be an important factor that determines the discrepancy between regional and local estimates of NEE.

Analysis of carbon isotope ratios of atmospheric CO_2 provides information with respect to underlying surface sources and plant processes. The carbon isotope ratios associated with net CO_2 fluxes ranged between -14 and $-9‰$ between June and August, reflecting the dominance of C_4 photosynthesis in the region. The spring-summer transition of $\delta^{13}C_{net}$ values suggested this grassland becoming progressively more dominated by C_4 grasses, which is exactly what we would expect based on C_3/C_4 productivity models and consistent with the ecosystem-scale work (Lai et al., 2003; 2006; Still et al., 2003; Griffis et al., 2005). The current analysis suggested a regional transition from C_3 to C_4 dominance, which has the potential to monitor region-wide shifts in productivity across the Great Plains of North America. $\delta^{13}C$ signatures in winter were much more variable, partially due to smaller CO_2 differences between the surface layer and the free troposphere (Fig. 2). The very negative $\delta^{13}C$ values in winter were probably due to the combustion of methane-originated fossil fuels in the area. The slower turnover of the surface boundary layer also likely contributes to the depleted $\delta^{13}C$ values. Other possibilities that could explain the seemingly over-negative $\delta^{13}C$ values include an invalid assumption of using a one-parameter fit model if both biological and fossil fuel fluxes contribute equally in winter, although this may seem unlikely.

We demonstrate in this study that subsampling CO_2 mixing ratios at midday in the surface layer can successfully derive regional net CO_2 fluxes over grassland. Our study differentiates from previous studies in several aspects: (1) we use flask-based mixing ratio measurements; (2) only discrete midday CO_2 mixing ratio data were used to construct time-series of CO_2 gradient between free troposphere and the ABL and (3) we propose a new means for estimating monthly averages of vertical transport between the free troposphere and the ABL, which also considers seasonal variations in the boundary layer height. Stable isotope analysis provides additional insight into integrated effects of surface sources and plant processes on atmospheric CO_2 over a large spatial scale.

5. Acknowledgements

We thank the two anonymous reviewers for their useful comments that improve the quality of this work. This research was supported through the Terrestrial Carbon Processes (TCP) program by the office of Science (BER), U.S. Department of Energy under Grant No. DE-FG03-00ER63012, and partially through the Great Plains Regional Center of the National Institute for Global Environmental Change (NIGEC) under Cooperative Agreement No. DE-FC03-90ER61010 and Grant No. FG03-99ER62863/A002. Financial support does not constitute an endorsement by DOE of the views expressed in this article. The authors would like to thank Lisa Auen for field assistance with air sample collection. Paul C. Novelli kindly provided carbon monoxide mixing ratio data from the Southern Great Plains Station, Oklahoma, USA within the NOAA/CMDL network. We are grateful to Craig Cook, Mike Lott, Shela Patrickson, W. Ike, J. Barleycorn, S. Bush and M. Moody for stable isotope analyses in the laboratory.

References

Bakwin, P. S., Davis, K. J., Yi, C., Wofsy, S. C., Munger, J. W. and co-authors. 2004. Regional carbon dioxide fluxes from mixing ratio data. *Tellus* **56B**, 301–311.

Bakwin, P. S., Tans, P. P., Hurst, D. F. and Zhao, C. 1998a. Measurements of carbon dioxide on very tall towers: results of the NOAA/CMDL program. *Tellus* **50B**, 401–415.

Bakwin, P. S., Tans, P. P., White, J. W. C. and Andres, R. J. 1998b. Determination of the isotopic ($^{13}C/^{12}C$) discrimination by terrestrial biology from a global network of observations. *Global Biogeochem. Cycles* **12**(3), 555–562.

Baldocchi, D. D. 1992. A Lagrangian random-walk model for simulating water vapor, CO_2 and sensible heat flux densities and scalar profiles over and within a soybean canopy. *Boundary Layer Meteorol.* **61**, 113–144.

Baldocchi, D. D. and Meyers, T. 1998. On using uco-physiological, uicrometeorological and uiogeochemical uheory to uvaluate carbon dioxide, water vapor and trace gas fluxes over vegetation: a perspective. *Agric. For. Meteorol.* **90**, 1–25.

Battle, M., Bender, M. L., Tans, P. P., White, J. W. C., Ellis, J. E. and co-authors. 2000. Global carbon sinks and their variability inferred from atmospheric O_2 and $\delta^{13}C$. *Science* **287**, 2467–2470.

Betts, A. K. 1992. FIFE atmospheric boundary layer budget methods. *J. Geophys. Res.* **97**, 18 523–18 532.

Betts, A. K. 2000. Idealized model for equilibrium boundary layer over land. *J. Hydrometeorol.* **1**, 507–523.

Betts, A. K. and Ridgeway, W. L. 1989. Climatic equilibrium of the atmospheric convective boundary layer over a tropical ocean. *J. Atmos. Sci.* **46**, 2621–2641.

Betts, A. K., Helliker, B. R. and Berry, J. A. 2004. Coupling between CO_2, water vapor, temperature, and radon and their fluxes in an idealized equilibrium boundary layer over land. *J. Geophys. Res.* **109**, D18103, doi:10.1029/2003JD004420.

Bousquet, P., Peylin, P., Ciais, P., Le Quéré, C., Friedlingstein, P. and co-authors. 2000. Regional changes in carbon dioxide fluxes of land and oceans since 1980. *Science* **290**, 1342–1346.

Bowling, D. R., Cook, C. S. and Ehleringer, J. R. 2001. Technique to measure CO_2 mixing ratio in small flasks with a bellows/IRGA system. *Agric. For. Meteorol.* **109**, 61–65.

Bremer, D. J., Ham, J. M., Owensby, C. E. and Knapp, A. K. 1998. Responses of soil respiration to clipping and grazing in a tallgrass prairie. *J. Environ. Qual.* **27**, 1539–1548.

Ciais, P., Tans, P. P., Trolier, M., White, J. W. C. and Francey, R. J. 1995. A large northern hemisphere terrestrial CO_2 sink indicated by the $^{13}C/^{12}C$ ratio of atmospheric CO_2. *Science* **269**, 1098–1102.

Conway, T. J., Tans, P. P., Waterman, L. S., Thoning, K. W., Kitzis, D. R. and co-authors. 1994. Evidence for interannual variability of the carbon cycle for the National Oceanic and Atmospheric Administration/Climate Monitoring Diagnostics Laboratory Global Air Sampling Network. *J. Geophys. Res.* **99**, 22 831–22 855.

Coplen, T. B. 1996. New guidelines for reporting stable hydrogen, carbon, and oxygen isotope-ratio data. *Geochim. Cosmochim. Acta* **60**, 3359–3360.

Cotton, W. R., Alexander, G. D., Hertenstein, R., Walko, R. L., McAnelly, R. L. and co-authors. 1995. Cloud venting: a review and some new global annual estimates. *Earth Sci. Rev.* **39**, 169–206.

Craine, J. M., Wedin, D. A. and Chapin, F. S., III. 1999. Predominance of ecophysiological controls on soil CO_2 flux in a Minnesota grassland. *Plant Soil* **207**, 77–86.

Davis, K. J. 2005. Well-calibrated CO_2 mixing ratio measurements at flux towers: The virtual tall towers approach. In: *12th WMO/IAEA meeting of experts on carbon dioxide concentration and related tracers measurement techniques*, No. 161, pp. 101–108, Toronto, Canada, 15–18 September, 2003.

Davis, K. J., Yi, C., Berger, B. W., Kubesh, R. J. and Bakwin, P. S. 2000. Scalar budgets in the continental boundary layer. In: *Proceedings of the 14th Symposium on Boundary Layer and Turbulence, 7–11 August*, American Meteorological Society, Aspen, CO, pp. 100–103.

Denmead, O. T., Raupach, M. R., Danin, F. X., Cleugh, H. A. and Leuning, R. 1996. Boundary layer budgets for regional estimates of scalar fluxes. *Global Change Biol.* **2**, 275–285.

ECMWF ERA-40 data used in this study/project have been provided by ECMWF/have been obtained from the ECMWF data server.

Fan, S.-M., Gloor, M., Mahlman, J., Pacala, S., Sarmiento, J. L. and co-authors. 1998. A large terrestrial carbon sink in North America implied by atmospheric and oceanic CO_2 data and models. *Science* **282**, 442–446.

Falge, E., Baldocchi, D., Olson, R., Anthoni, P., Aubinet, M. and co-authors. 2001. Gap filling strategies for defensible annual sums of net ecosystem exchange. *Agric. For. Meteorol.* **107**, 43–69.

Farquhar, G. D., Ehleringer, J. R. and Hubick, K. T. 1989. Carbon isotope discrimination and photosynthesis. *Annu. Rev. Physiol. Plant Mol. Biol.* **40**, 503–537.

Fitzjarrald, D. R. 2004. Boundary layer budgeting. In: *Vegetation, Water, Humans and the Climate: A New Perspective on an Interactive System* (eds. Kabat, P. C., Claussen, M., Dirmeyer, P. A., Gash, J. H. C. and Guenni, L. B. et al.). Springer-Verlag, New York, pp. 189–196.

Fung, I., Field, C. B., Berry, J. A., Thompson, M. V., Randerson, J. T. and co-authors. 1997. Carbon 13 exchanges between the atmosphere and the biosphere. *Global Biogeochem. Cycles* **11**, 507–533.

GLOBALVIEW-CO2. 2003. Cooperative Atmospheric Data Integration Project – Carbon Dioxide. CD-ROM, NOAA CMDL, Boulder, Colorado [Also available on Internet via anonymous FTP to ftp.cmdl.noaa.gov, Path: ccg/co2/GLOBALVIEW].

Gloor, M., Bakwin, P., Hurst, D., Lock, L., Draxler, R. and co-authors. 2001. What is the concentration footprint of a tall tower? *J. Geophys. Res.* **106**, 17 831–17 840.

Griffis, T. J., Baker, J. M. and Zhang, J. 2005. Seasonal dynamics and partitioning of isotopic CO_2 exchange in a C_3/C_4 managed ecosystem. *Agric. For. Meteorol.* **132**, 1–19.

Gurney, K. R., Law, R. M., Denning, A. S., Rayner, P. J., Baker, D. and co-authors. 2002. Towards robust regional estimates of CO_2 sources and sinks using atmospheric transport models. *Nature* **415**, 626–630.

Ham, J. M. and Heilman, J. L. 2003. Experimental test of density and energy-balance corrections on CO_2 flux as measured using open-path eddy covariance. *Agron. J.* **95**, 1393–1403.

Helliker, B. R., Berry, J. A., Betts, A. K., Bakwin, P. S., Davis, K. J. and co-authors. 2005. Regional-scale estimates of forest CO_2 and isotope flux based on monthly CO_2 budgets of the atmospheric boundary layer. In: *The Carbon Balance of Forest Biomes* (eds.H. Griffiths and P. G. Jarvis). Taylor and Francis Group (Bios), New York, pp. 77–92.

Helliker, B. R., Berry, J. A., Betts, A. K., Bakwin, P. S., Davis, K. J. and co-authors. 2004. Estimates of net CO_2 flux by application of equilibrium boundary layer concepts to CO_2 and water vapor measurements from a tall tower. *J. Geophys. Res.* **109**, D20106, doi:10.1029/2004JD004532.

Hurwitz, M. D., Ricciuto, D. M., Davis, K. J., Wang, W., Yi, C. and co-authors. 2004. Advection of carbon dioxide in the presence of storm systems over a northern Wisconsin forest. *J. Atmos. Sci.* **61**, 607–618.

Kalnay, E., Kanamitsu, M., Kistler, R., Collins, W., Deaven, D. and co-authors. 1996. The NCEP/NCAR 40-year reanalysis project. *Bull. Am. Meteorol. Soc.* **77**, 437–471.

Keeling, C. D., Chin, J. F. S. and Whorf, T. P. 1996. Increased activity of northern vegetation inferred from atmospheric CO_2 measurements. *Nature* **382**, 146–148.

Kuck, L. R., Smith, T., Balsley, B. B., Helmig, D., Conway, T. J. and co-authors. 2000. Measurements of landscape-scale fluxes of carbon dioxide in the Peruvian Amazon by vertical profiling through the atmospheric boundary layer. *J. Geophys. Res.* **105**, 22 137–22 146.

Lai, C.-T., Katul, G., Ellsworth, D. S. and Oren, R. 2000a. Modeling vegetation-atmosphere CO_2 exchange by a coupled Eulerian-Lagrangian approach. *Boundary Layer Meteorol.* **95**, 91–12.

Lai, C.-T., Katul, G., Oren, R., Ellsworth, D. and Schäfer, K. 2000b. Modeling CO_2 and water vapor turbulent flux distributions within a forest canopy. *J. Geophys. Res.* **105**(D21), 26 333–26 351.

Lai, C.-T., Ehleringer, J. R., Schauer, A. J., Tans, P. P., Hollinger, D. Y. and co-authors. 2005. Canopy-scale $\delta^{13}C$ of photosynthetic and respiratory CO_2 fluxes: observations in forest biomes across the United States. *Global Change Biol.* **11**, 633–643, doi:10.1111/j.1365–2486.2005.00931.x.

Lai, C.-T., Ehleringer, J. R., Tans, P. P., Wofsy, S. C., Urbanski, S. P. and co-authors. 2004. Estimating photosynthetic ^{13}C discrimination in terrestrial CO_2 exchange from canopy to regional scales. *Global Biogeochem. Cycles* **18**, GB1041, doi:10.1029/2003GB002148.

Lai, C.-T., Riley, W., Owensby, C., Ham, J., Schauer, A. and co-authors. 2006. Seasonal and interannual variations of carbon and oxygen isotopes of respired CO_2 in a tallgrass prairie: Measurements and modeling results from 3 years with contrasting water availability. *J. Geophys. Res.* **111**, D08S06, doi:10.1029/2005JD006436.

Lai, C.-T., Schauer, A. J., Owensby, C., Ham, J. M. and Ehleringer, J. R. 2003. Isotopic air sampling in a tallgrass prairie to partition net ecosystem CO_2 exchange. *J. Geophys. Res.* **108**(D18), 4566, doi:10.1029/2002JD003369.

Levy, P. E., Grelle, A., Lindroth, A., Molder, M., Jarvis, P. G. and co-authors. 1999. Regional-scale CO_2 fluxes over central Sweden by a boundary layer budget method. *Agric. For. Meteorol.* **99**, 169–180.

Lloyd, J., Francey, R. J., Mollicone, D., Raupach, M. R. and Sogachev, A. 2001. Vertical profiles, boundary layer budgets, and regional flux estimates for CO_2 and its $^{13}C/^{12}C$ ratio and for water vapor above a forest/bog mosaic in central Siberia. *Global Biogeochem. Cycles* **15**, 267–284.

Masarie, K. A. and Tans, P. P. 1995. Extension and integration of atmospheric carbon dioxide data into a globally consistent measurement record. *J. Geophys. Res.* **100**(D6), 11 593–11 610.

Moeng, C.-H. and Wyngaard, J. C. 1989. Evaluation of turbulent and dissipation closures in second-order modeling. *J. Atmos. Sci.* **45**, 2311–2330.

Potosnak, M. J., Wofsy, S. C., Denning, A. S., Conway, T. J., Munger, J. W. and co-authors. 1999. Influence of biotic exchange and combustion sources on atmospheric CO_2 concentration in New England from observations at a forest flux tower. *J. Geophys. Res.* **104**, 9561–9569.

Raupach, M. R. 1989a. A practical Lagrangian method for relating scalar concentrations to source distributions in vegetation canopies. *Q. J. R. Meteorol. Soc.* **115**, 609–632.

Raupach, M. R. 1989b. Applying Lagrangian fluid mechanics to infer scalar source distributions from concentration profiles in plant canopies. *Agric. For. Meteorol.* **47**, 85–108.

Raupach, M. R., Denmead, O. T. and Dunin, F. X. 1992. Challenges in linking atmospheric CO_2 concentrations to fluxes at local and regional scales. *Aust. J. Bot.* **40**, 697–716.

Rayner, P. J., Enting, I. G., Francey, R. J. and Langenfields, R. 1999. Reconstructing the recent carbon cycle from atmospheric CO_2, $\delta^{13}C$ and O_2/N_2 observations. *Tellus* **51B**, 213–232.

Schauer, A. J., Lai, C.-T., Bowling, D. R. and Ehleringer, J. R. 2003. An automated sampler for collection of atmospheric trace gas samples for stable isotope analyses. *Agric. For. Meteorol.* **118**, 113–124.

Schauer, A. J., Lott, M. J., Cook, C. S. and Ehleringer, J. R. 2005. An automated system for stable isotope and concentration analyses of CO_2 from small atmospheric samples. *Rapid Commun. Mass Spectrom.* **19**, 359–362, doi:10.1002/rem.1792.

Schimel, D. S., Braswell, B. H., Holland, E. A., McKeown, R., Ojima, D. S. and co-authors. 1994. Climatic, edaphic, and biotic controls over storage and turnover of carbon in soils. *Global Biogeochem. Cycles* **8**, 279–293.

Siqueira, M., Katul, G. and Lai, C.-T. 2002. Quantifying net ecosystem exchange by multilevel ecophysiological and turbulent transport models. *Adv. Water Res.* **25**, 1357–1366.

Still, C. J., Berry, J. A., Ribas-Carbó, M. and Helliker, B. R. 2003. The contribution of C_3 and C_4 plants to the carbon cycle of a tallgrass prairie: an isotopic approach. *Oecologia* **136**, 347–359.

Stull, R. B. 1988. *An Introduction to Boundary Layer Meteorology*. Kluwer Academic Publishers, pp. 666.

Styles, J. M., Lloyd, J., Zolotoukhine, D., Lawton, K. A., Tchebakova, N. and co-authors. 2002. Estimates of regional surface carbon dioxide exchange and carbon and oxygen isotope discrimination during photosynthesis from concentration profiles in the atmospheric boundary layer. *Tellus* **54B**, 768–783.

Suyker, A. E. and Verma, S. B. 2001. Year-round observations of the net ecosystem exchange of carbon dioxide in a native tallgrass prairie. *Global Change Biol.* **7**, 279–289.

Tans, P. P., Fung, I. Y. and Takahashi, T. 1990. Observational constraints on the global atmospheric CO_2 budget. *Science* **247**, 1431–1438.

Thoning, K. W., Tans, P. P. and Komhyr, W. D. 1989. Atmospheric carbon dioxide at Mauna Loa observatory 2. Analysis of the NOAA GMCC data, 1974–1985. *J. Geophys. Res.* **94**, 8549–8565.

Trolier, M., White, J. W. C., Tans, P. P., Masarie, K. A. and Gemery, P. A. 1996. Monitoring the isotopic composition of atmospheric CO_2: measurements from the NOAA Global Air Sampling Network. *J. Geophys. Res.* **101**, 25 897–25 916.

Wofsy, S. C., Harriss, R. C. and Kaplan, W. A. 1988. Carbon dioxide in the atmosphere over the Amazon basin. *J. Geophys. Res.* **93**, 1377–1388.

Yi, C., Davis, K. J., Bakwin, P. S., Denning, A. S., Zhang, N. and co-authors. 2004. The observed covariance between ecosystem carbon exchange and atmospheric boundary layer dynamics in North Wisconsin,. *J. Geophys. Res.* **109**(D08302), doi10.1029/2003JD004164.

Yi, C., Davis, K. J., Bakwin, P. S. and Berger, B. W. 2001. Long-term observations of the evolution of the planetary boundary layer. *J. Atmos. Sci.* **58**, 1288–1299.